SUPPLEMENTARY MATERIAL

A. Radiative transfer equation for QPAT

For QPAT, the time-independent RTE in $r \in \Omega \subset \mathbb{R}^n$ ($n = 2$ or 3) with given scattering μ_s and absorption μ_a coefficients can be written as [1]

$$\begin{aligned} &\hat{s} \cdot \nabla \phi(r, \hat{s}) + (\mu_s + \mu_a)\, \phi(r, \hat{s}) \\ &= \mu_s \int_{S^{n-1}} \Theta\left(\hat{s} \cdot \hat{s}'\right) \phi\left(r, \hat{s}'\right) \mathrm{d}\hat{s}' + q(r, \hat{s}), \quad r \in \Omega, \end{aligned} \tag{1}$$

where $\Theta\left(\hat{s} \cdot \hat{s}'\right)$ is the scattering phase function and $q(r, \hat{s})$ is the source in Ω, $\partial\Omega$ is the domains boundary, and $\hat{s} \in S^{n-1}$ denotes a unit vector in the direction of interest. With the radiance $\phi(r, \hat{s})$, we can compute the photon fluence as $\Phi(r) = \int_{S^{n-1}} \phi(r, \hat{s}) \mathrm{d}\hat{s}$

For modeling biological tissues, the scattering phase function is commonly chosen to be the Henyey–Greenstein scattering function [2]. For QPAT, the boundary condition of RTE is often formed by assuming that at the boundary $\partial\Omega$, photons travel in an inward direction only at the source positions.

B. Diffusion approximation and finite element matrices

By choosing Henyey–Greenstein scattering function [2] and assuming a diffusive region $r \in \Omega \subset \mathbb{R}^n$ ($n = 2$ or 3) with absorption μ_a and scattering μ_s coefficients, the diffusion approximation of RTE (1) is given by (see e.g. [3])

$$-\nabla \cdot \kappa(r) \nabla \Phi(r) + \mu_a(r) \Phi(r) = q_0(r), \quad r \in \Omega,$$

where q_0 is the light source in Ω, the parameter $\kappa(r) = (n(\mu_a(r) + \mu_s'(r)))^{-1}$ is the diffusion coefficient where $\mu_s' = (1-g)\mu_s$ is the reduced scattering coefficient with anisotropy parameter $-1 < g < 1$. A boundary condition for the DA can be formed by assuming that the total inward-directed photon current is zero at the boundary. Moreover, including the possible refraction mismatch between Ω and its surrounding medium, the boundary condition for DA can be derived to be [3]

$$\Phi(r) + \frac{1}{2\gamma} \kappa(r) A \frac{\partial \Phi(r)}{\partial \hat{n}} = \begin{cases} \frac{I(r)}{\gamma}, & r \in \rho \\ 0, & r \in \partial\Omega \backslash \rho, \end{cases},$$

where $\hat{n}$ is the outward unit normal vector, $I(r)$ is the boundary photon flux at the source positions $\rho \in \partial\Omega, \gamma$ is a dimension-dependent constant with values $1/\pi$ in $\mathbb{R}^2$ and 1/4 in $\mathbb{R}^3$. The parameter A accounts for the internal reflection at the boundary $\partial\Omega$. If no boundary refraction occurs, A corresponds to 1.

Assume that the domain is separated into P non-overlapping elements with N grid coordinates, and that the optical parameters in Ω are represented as

$$\mu_a(r) \approx \sum_{t=1}^{N} \mu_{a_t} \varphi_t(r), \quad \mu_s(r) \approx \sum_{t=1}^{N} \mu_{s_t} \varphi_t(r), \tag{2}$$

with the chosen finite element basis φ_t. The finite element approximation for the diffusion approximation can then be written as

$$(M + C + R)\Phi = Q,$$

where

$$\begin{aligned} M(i,j) &= \sum_{t=1}^{N} \frac{1}{n(\mu_{a_t} + \mu_{s_t}')} \int_\Omega \varphi_t(r) \nabla \varphi_i(r) \cdot \nabla \varphi_j(r) \mathrm{d}r \\ C(i,j) &= \sum_{t=1}^{N} \mu_{a_t} \int_\Omega \varphi_t(r) \varphi_i(r) \varphi_j(r) \mathrm{d}r \\ R(i,j) &= \int_{\partial\Omega} \frac{2\gamma}{A} \varphi_i(r) \varphi_j(r) \mathrm{d}S \\ Q(i) &= \int_{\partial\Omega} \frac{2I(r)}{A} \varphi_i(r) \mathrm{d}S. \end{aligned}$$

C. Distribution of simulated optical coefficients

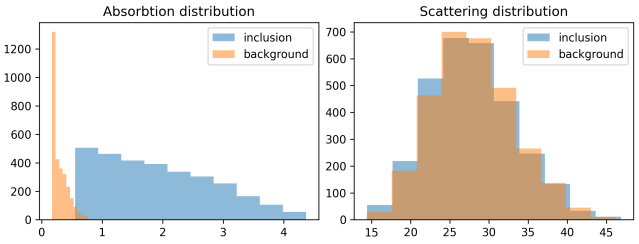

Fig. S1. *Digital twin problem*: Distribution of the simulated absorption coefficient (left) and scattering coefficient (right) values for both the background material (orange) and the inclusion materials (blue). While there is a distinct difference between the background and inclusion materials on the absorption values, there is no difference in the scattering distribution. The y-axes shows the bin frequencies when drawing 10,000 samples. The x-axes show the absorption and scattering coefficient in units of cm^{-1}.

D. Reconstructions from time-series data

Here, we present a few additional test reconstructions from the time-series data. Reconstructions of the acoustic problem have been obtained from the corresponding variational problem with TV regularization solved using the primal-dual hybrid gradient, as discussed in [4]. The optical problem was solved using the U-Net and a learned iterative Gauss-Newton solver (Learned GN). Figs. S2 and S3 show reconstructions from both solvers.

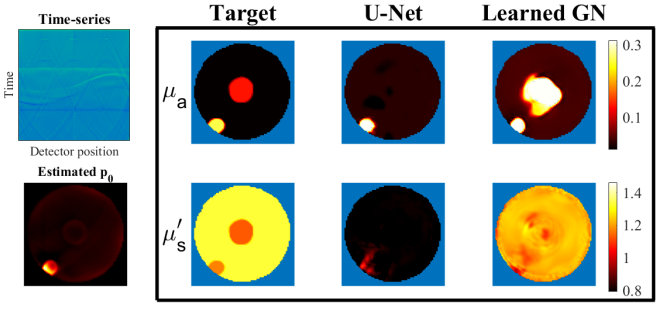

Fig. S2. Absorption (μ_a) and reduced scattering (μ_s') reconstructions of a test sample solved from experimental time-series data. The left-most column shows an initial acoustic field p_0 (bottom) that is estimated from the shown time-series (top) using a classical iterative solver.

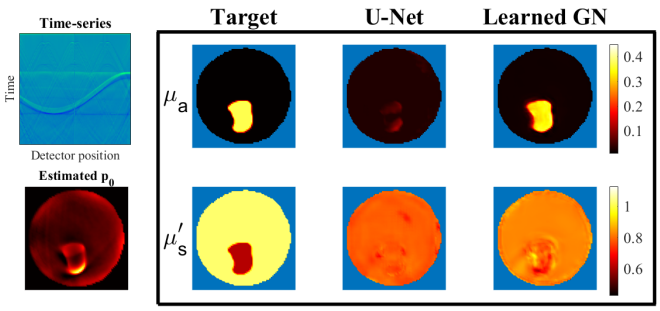

Fig. S3. Absorption (μ_a) and reduced scattering (μ_s') reconstructions of a test sample solved from experimental time-series data. The left-most column shows an initial acoustic field p_0 (bottom) that is estimated from the shown time-series (top) using a classical iterative solver.

REFERENCES

[1] A. Ishimaru *et al.*, *Wave propagation and scattering in random media*. Academic press New York, 1978, vol. 2.

[2] L. G. Henyey and J. L. Greenstein, "Diffuse radiation in the galaxy," *Astrophysical Journal, vol. 93, p. 70-83 (1941).*, vol. 93, pp. 70–83, 1941.

[3] S. R. Arridge, "Optical tomography in medical imaging," *Inverse problems*, vol. 15, no. 2, p. R41, 1999.

[4] A. Hauptmann, L. Kunyansky, and J. Poimala, "Fast algorithms enabling optimization and deep learning for photoacoustic tomography in a circular detection geometry," *SIAM Journal on Imaging Sciences*, 2026.